MESOMETEOROLOGY PROJECT

Department of the Geophysical Sciences
The University of Chicago

DEVELOPMENT OF A DRY LINE AS SHOWN BY ATS CLOUD PHOTOGRAPHY AND VERIFIED BY RADAR AND CONVENTIONAL AEROLOGICAL DATA

by

Dorothy L. Bradbury

The University of Chicago

Number 80

November 1969

MESOMETEOROLOGY PROJECT --- RESEARCH PAPERS

1.* Report on the Chicago Tornado of March 4, 1961 - Rodger A. Brown and Tetsuya Fujita

2.* Index to the NSSP Surface Network - Tetsuya Fujita

3.* Outline of a Technique for Precise Rectification of Satellite Cloud Photographs - Tetsuya Fujita

4.* Horizontal Structure of Mountain Winds - Henry A. Brown

5.* An Investigation of Developmental Processes of the Wake Depression Through Excess Pressure Analysis of Nocturnal Showers - Joseph L. Goldman

6.* Precipitation in the 1960 Flagstaff Mesometeorological Network - Kenneth A. Styber

7.** On a Method of Single- and Dual-Image Photogrammetry of Panoramic Aerial Photographs - Tetsuya Fujita

8. A Review of Researches on Analytical Mesometeorology - Tetsuya Fujita

9.* Meteorological Interpretations of Convective Nephsystems Appearing in TIROS Cloud Photographs - Tetsuya Fujita, Toshimitsu Ushijima, William A. Hass, and George T. Dellert, Jr.

10.* Study of the Development of Prefrontal Squall-Systems Using NSSP Network Data - Joseph L. Goldman

11. Analysis of Selected Aircraft Data from NSSP Operation, 1962 - Tetsuya Fujita

12. Study of a Long Condensation Trail Photographed by TIROS I - Toshimitsu Ushijima

13. A Technique for Precise Analysis of Satellite Data; Volume I - Photogrammetry (Published as MSL Report No. 14) - Tetsuya Fujita

14. Investigation of a Summer Jet Stream Using TIROS and Aerological Data - Kozo Ninomiya

15. Outline of a Theory and Examples for Precise Analysis of Satellite Radiation Data - Tetsuya Fujita

16. Preliminary Result of Analysis of the Cumulonimbus Cloud of April 21, 1961 - Tetsuya Fujita and James Arnold

17. A Technique for Precise Analysis of Satellite Photographs - Tetsuya Fujita

18.* Evaluation of Limb Darkening from TIROS III Radiation Data - S.H.H. Larsen, Tetsuya Fujita, and W.L. Fletcher

19. Synoptic Interpretation of TIROS III Measurements of Infrared Radiation - Finn Pedersen and Tetsuya Fujita

20.* TIROS III Measurements of Terrestrial Radiation and Reflected and Scattered Solar Radiation - S.H.H. Larsen, Tetsuya Fujita, and W.L. Fletcher

21. On the Low-level Structure of a Squall Line - Henry A. Brown

22.* Thunderstorms and the Low-level Jet - William D. Bonner

23.* The Mesoanalysis of an Organized Convective System - Henry A. Brown

24. Preliminary Radar and Photogrammetric Study of the Illinois Tornadoes of April 17 and 22, 1963 - Joseph L. Goldman and Tetsuya Fujita

25. Use of TIROS Pictures for Studies of the Internal Structure of Tropical Storms - Tetsuya Fujita with Rectified Pictures from TIROS I Orbit 125, R/O 128 - Toshimitsu Ushijima

26. An Experiment in the Determination of Geostrophic and Isallobaric Winds from NSSP Pressure Data - William Bonner

27. Proposed Mechanism of Hook Echo Formation - Tetsuya Fujita with a Preliminary Mesosynoptic Analysis of Tornado Cyclone Case of May 26, 1963 - Tetsuya Fujita and Robbi Stuhmer

28. The Decaying Stage of Hurricane Anna of July 1961 as Portrayed by TIROS Cloud Photographs and Infrared Radiation from the Top of the Storm - Tetsuya Fujita and James Arnold

29. A Technique for Precise Analysis of Satellite Data, Volume II - Radiation Analysis, Section 6. Fixed-Position Scanning - Tetsuya Fujita

30. Evaluation of Errors in the Graphical Rectification of Satellite Photographs - Tetsuya Fujita

31. Tables of Scan Nadir and Horizontal Angles - William D. Bonner

32. A Simplified Grid Technique for Determining Scan Lines Generated by the TIROS Scanning Radiometer - James E. Arnold

33. A Study of Cumulus Clouds over the Flagstaff Research Network with the Use of U-2 Photographs - Dorothy L. Bradbury and Tetsuya Fujita

34. The Scanning Printer and Its Application to Detailed Analysis of Satellite Radiation Data - Tetsuya Fujita

35. Synoptic Study of Cold Air Outbreak over the Mediterranean using Satellite Photographs and Radiation Data - Aasmund Rabbe and Tetsuya Fujita

36. Accurate Calibration of Doppler Winds for their use in the Computation of Mesoscale Wind Fields - Tetsuya Fujita

37. Proposed Operation of Intrumented Aircraft for Research on Moisture Fronts and Wake Depressions - Tetsuya Fujita and Dorothy L. Bradbury

38. Statistical and Kinematical Properties of the Low-level Jet Stream - William D. Bonner

39. The Illinois Tornadoes of 17 and 22 April 1963 - Joseph L. Goldman

40. Resolution of the Nimbus High Resolution Infrared Radiometer - Tetsuya Fujita and William R. Bandeen

41. On the Determination of the Exchange Coefficients in Convective Clouds - Rodger A. Brown

* Out of Print
** To be published

(Continued on back cover)

SATELLITE AND MESOMETEOROLOGY RESEARCH PROJECT

Department of the Geophysical Sciences

The University of Chicago

DEVELOPMENT OF A DRY LINE AS SHOWN BY ATS CLOUD PHOTOGRAPHY AND VERIFIED BY RADAR AND CONVENTIONAL AEROLOGICAL DATA

by

Dorothy L. Bradbury

The University of Chicago

SMRP Research Paper No. 80

November 1969

The research reported in this paper was sponsored by the U. S. Weather Bureau, ESSA under grants E-41-22-69-(G) and E-198-68-(G).

DEVELOPMENT OF A DRY LINE AS SHOWN BY ATS CLOUD PHOTOGRAPHY AND VERIFIED BY RADAR AND CONVENTIONAL AEROLOGICAL DATA[1]

by

Dorothy L. Bradbury

The University of Chicago

ABSTRACT

A series of ATS-III cloud pictures taken on 19 April 1968 shows the formation, development, and movement of a dry line. The line was detected on the ATS-III pictures long before it was observed on the radar screen and its development and motion was observed on consecutive ATS-III pictures at 14 min intervals over a period of six and one-half hours.

A vertical cross-section through the dry dome shows that the isentropic layer extended up to the 500 mb surface and that the dry line was nearly vertical up to this height. The vertical distribution of the horizontal winds in the cross-section indicate jet maxima at three different levels, at and above the 600 mb surface, in addition to the low level jet located between 800 and 900 mb. The jet maxima most closely associated with the intense convective activity appears to be centered between 600 and 500 mb.

1. Introduction

In the spring of 1968 a Tornado Watch Experiment was conducted with the cooperation of NASA and ESSA. The principal investigators were Professor V. Suomi of the University of Wisconsin, Professor T. T. Fujita of the University of Chicago, and Mr. V. Oliver of NESC. On days when tornado and/or severe storm activity was expected over the midwest the ATS-III was programmed to take half-scan pictures from the North Pole to the equator during each cycle, thus producing a cloud picture about every 14 minutes. This interval between pictures is very useful for the study of mesoscale systems such as squall lines, thunderstorm activity, and other small scale meteorological phenomena.

---

[1]The research reported in this paper has been supported by the U.S. Weather Bureau, ESSA, under grants E-41-22-69-(G) and E-198-68-(G).

One day on which tornado activity was forecast was 19 April 1968. Scattered tornado activity did occur over eastern Oklahoma during the afternoon, but the most intense and destructive tornado passed through Greenwood, Arkansas around 1512 CST. Unfortunately, it was not possible to identify any single cloud element or cloud mass associated with this specific system because of the solid cloud cover over the entire area of thunderstorm activity.

However, one significant feature on the series of ATS-III cloud pictures was a distinct line of convective clouds observed over the western Texas-Oklahoma Panhandle region which could be followed throughout an entire series of 29 pictures. This feature is often observed originating along the eastern slopes of the Rocky Mountains, especially over eastern Colorado and New Mexico, western Kansas and Nebraska and the Texas-Oklahoma panhandle area. As the air moves over the Rocky Mountains the subsiding air becomes extremely dry. Under clear skies the air is rapidly warmed and dew-point temperatures become very low. As this mass of air moves eastward a line of convection forms between the mass of dry air and the more moist air ahead of it. The intensity of the convection varies with individual cases; some develop into very severe thunderstorms accompanied by tornadoes while others grow into thunderstorms of moderate intensity and weaken during the late afternoon as the solar heating decreases. The development of such lines and the direction and rate of their movement is of interest to forecasters in the Great Plains states and to aircraft operations in the area.

Beebe (1958) described the development of such dry lines or fronts and Fujita (1958) described their structure and movement. Both used data obtained from three aircraft flights on 11 June 1956. During the spring and summer of 1956 the Tornado Research Aircraft of the U. S. Weather Bureau flew over and within such dry lines on days when convective activity was predicted. Observers on the aircraft were able to detect the first convective clouds soon after they formed, long before the clouds reached the stage of development to produce echoes that could be detected by radar. McGuire (1962) used aircraft data from two flights in 1959 and one in 1960 to determine the vertical structure of such fronts. He found these fronts to be nearly vertical and the dew point gradient across the line was nearly constant from the ground to the 700-mb surface.

On a TIROS IX photograph taken at 1242 CST on 11 April 1965 Fujita (1966) observed a cloud free dome of dry air over Oklahoma, Kansas, and Missouri. Soon after the TIROS IX picture was taken the first tornado touchdown was reported over northeast Iowa and the convective activity spread eastward as the dry front advanced, with the most intense activity occurring over Indiana, southern Michigan and Ohio between 1600 and 1900 CST.

It is the purpose of this paper to show that ATS-III cloud pictures can be used to detect dry lines soon after they develop, long before they can be picked up by radar and to follow their locations on consecutive frames to determine their motion and development. The ATS-III pictures were combined with conventional surface and upper-air data to study the three dimensional structure of the cool dry dome and to verify the development and movement of the dry line.

2. Synoptic situation

Early on 19 April 1968 the surface chart showed a weak low pressure center located over eastern New Mexico that was moving slowly northeastward. Very moist, stable, tropical Gulf air covered that part of the United States east of 100 W and south of 35 N. Haze and fog were reported at nearly every station in the area. A large continental anticyclone, centered over James Bay, dominated the northern part of the United States with a weak, diffuse warm front separating the air masses of polar and tropical origin. Overrunning of moist Gulf air resulted in widespread fog, drizzle and occasional light shower activity north of the front and in the frontal zone.

By 1200 CST (fig. 1) the weak low pressure center had become more organized, and a low pressure of 1001 mb was reported over southeastern Colorado. As the center moved northeastward away from the Rocky Mountains the subsiding air brought in behind it became very dry. This is indicated by the large, nearly cloud-free tongue over eastern New Mexico and along the border of the Texas panhandle.

At 1500 CST (fig. 2) the 999 mb low pressure center was located over southwestern Kansas and the dry tongue had moved eastward across west Texas, spreading over the Texas and Oklahoma Panhandle region. Severe thunderstorm activity was reported

in northwest Arkansas at this time. During the afternoon there were six reported tornadoes over eastern Oklahoma, with the severest one touching down at 1430 CST near the Oklahoma-Arkansas border and passing through Greenwood, Arkansas around 1512 CST. As can be seen from fig. 2 this activity was far in advance of the dry front.

Figure 3 shows that by 1800 CST the low pressure center was located over south-central Kansas and had deepened to 996 mb. The dry air tongue had spread northeastward to Garden City and Dodge City, Kansas and as far eastward as Gage, Oklahoma and Childress, Texas.

Figures 4, 5, and 6 show the isodrosotherm patterns superimposed upon the ATS-III pictures for 1200, 1500, and 1800 CST, respectively. At 1200 CST a wind shift line separates the Moist Gulf air (dewpoints 14 to 20 C) from the modified continental air (dewpoints 2 to 10 C). The modified continental was transported into the region from an area east of the Rocky Mountains and had not undergone orographic subsidence. As can be seen in Fig. 1 the surface winds were blowing nearly parallel to the isodrosotherms in the modified continental air. This resulted in the strengthening of the dewpoint gradient and produced the dewpoint front (A-A) or dry line along the windshift line. To the rear of this line the low cloud cover dissipated and only broken to scattered middle type clouds were observed. Farther west as the very dry air advanced a line of convection (B-B) formed between the very dry air and the modified continental air. The low-level winds in this very dry air were strong and gusty and the dry dome was advancing at a rate of about 30 knots. By 1800 CST the two dewpoint fronts had merged to form a very strong dry front over central Oklahoma.

Figure 7 shows a time-section of pressure, temperature, dewpoint, cloud cover, and wind direction and speed between 0600 and 1800 CST for two reporting stations over which both dry lines passed during this time. The two stations are approximately 120 n mi apart and a line joining the two would lie almost parallel to the dry lines. Dry line A-A passed over station CDS between 1200 and 1300 CST accompanied by a drop in dewpoint of 5C and a shift in wind from south to southwesterly. The second line, B-B passed over the station after 1400 CST, with a rapid decrease in dewpoint temperature and an increase in wind speed, becoming gusty, and accompanied by blowing dust.

The lower part of fig. 7 shows that line A-A passed over station GAG between 1300 and 1400 CST accompanied by a dewpoint drop of 8.3 C and was followed by line B-B between 1500 and 1600 CST with a further drop of the dewpoint by another 9C. In both cases there was little change in the air temperature with the passage of the dry lines.

The development and structure of the dry line B-B will be discussed in detail.

3. Development and Movement of the Dry Line

The development and movement of the dry line B-B was observed on the series of twenty-nine consecutive frames (nos. 6-34) of the ATS-III cloud pictures. The period covered was from 1135 through 1804 CST or a period of 6 hours 29 minutes. Figure 8 shows the consecutive positions of the line of convection initiated by the dry line during the six and one half hour period.

At 1200 CST (Fig. 4) the dry line B-B was indicated by two areas of convection separated by a faint line of scattered cumulus about 90 n mi in length. One area of convection was located in the Texas panhandle area just southeast of Clovis, New Mexico and the other was just west of Amarillo, Texas. This latter cloud mass extended in a line northward through the Oklahoma panhandle to the Colorado border. No radar echoes were reported at the time of this picture. As the dry dome spread eastward and northeastward the line of convection intensified and by 1300 CST a distinct solid line of clouds could be observed on the ATS-III picture. As the line moved through Amarillo (AMA) the dew point temperatures dropped from 8.3 C at 1100 CST to 2.8 C at 1200 CST, and to -4.4 C at 1300 CST (see fig. 9). During the same period the cloud cover changed from scattered cumulus at 1100 feet to broken at 5000 feet to clear. The air temperature rose about 3.3 C between 1100 and 1200 CST and remained nearly constant until after 1800 CST. The dewpoint temperature continued to lower and reached its minimum of -17.2 C at 1400 CST and then began a gradual rise.

The dry line B-B advanced at a nearly steady rate and the band of convective clouds grew broader during its intensification. The distance between the two dewpoint fronts narrowed since line B-B was moving at a slightly faster rate than A-A. By 1800 CST the two lines had nearly merged, especially at the northern end and convective activity

had greatly intensified.

The first radar echo associated with dry line A-A was detected by the Oklahoma City radar about 1500 CST (fig. 5) and the Radar Summary issued by the Kansas City Severe Storms unit at 1445 CST indicated a thin line of light thundershower activity about 80 n mi west-northwest of OKC moving northeastward at 30 knots. One hour later, at 1545 CST, the radar summary indicated a wider band of echoes increasing in intensity with tops at 28,000 feet. By 1800 CST this dry line B-B had merged with dry-line A-A to form a very strong front. The radar echoes associated with this front are shown in fig. 6 and are indentified by the dark shaded area through central Oklahoma.

4. Vertical structure of the dry line

Using aircraft data from the 1956 flights Fujita (1958) determined that dry fronts or lines were nearly vertical or tilted slightly toward the east. McGuire (1962) arrived at the same conclusion when he used aircraft data obtained in flight operation in 1959 and 1960. Fujita (1966) constructed a chart showing the topography of the top of the dry dome by using conventional surface and upper air data combined with TIROS IX cloud pictures for the 11 April 1965 tornado case. He found that the dome extended up to above the 600-mb surface and that the isentropes at the leading edge formed a nearly vertical wall.

Dry front B-B observed in this case of 19 April 1968 differed from the formerly described cases in that it formed between the very dry air and the modified continental polar air that had not undergone orographic subsidence rather than between the very dry subsiding air and moist tropical air.

The upper part of fig. 9 shows the vertical temperature and dewpoint distributions at Amarillo, Texas (AMA) at 0600, 1200, and 1800 CST on April 19. The upper winds are indicated in the left margin with the numbers representing the speed in kts. At 0600 CST the sounding shows a strong inversion just above the ground about 3000 ft in thickness with relatively moist air above to about the 500-mb surface. With the rapid heating and vertical mixing during the late morning hours the low level inversion was replaced by an adiabatic layer about 5600 ft deep with θ = 298 K at 1200 CST. The 0600 CST

sounding shows advection of very moist air below the inversion and nearly zero wind speed shear in the unstable layer between 800 and 700 mb. The light drizzle and fog reported on the surface observations (lower chart) between the hours of 0600 and 0900 CST agrees with the upper air conditions indicated by the 0600 CST sounding. With the passage of the dry line B-B over AMA around 1200 CST dry air was advected at all levels below 500 mb and the cloud cover dissipated. The surface air temperature had reached its maximum (θ =300 K) by noonday and changed very little during the afternoon, even under clear skies. However, the dewpoint temperature continued to decrease, reaching a minimum of -17.2 C at 1400 CST. The 1800 CST sounding shows that as the result of vertical mixing in the lower levels and advection of cool dry air between 700 and 500 mb the air is nearly isentropic from the ground to about 18,000 ft. Within the dome the winds are nearly constant with height, indicating very little vertical wind shear. The isentropic layer is topped by a strong inversion of 5 C about 1500 ft in thickness and through this layer the winds increased from 48 knots to 84 knots.

A vertical cross-section between Little Rock, Arkansas (LIT) and Albuquerque, New Mexico (ABQ) at 1200 CST intercepts the dry line B-B near AMA. Shown in fig. 10 is the vertical temperature distribution and the isentropic analysis. Since ABQ was not scheduled for a special radiosonde at this hour, the vertical pressure-temperature distribution was interpolated from its 0600 and 1800 CST soundings. As can be seen, in the moist tropical air the isentropes below the 850-mb surface are parallel to the slope of the topography eastward from Amarillo. To the west of AMA the 298 K isentrope is near the 630 mb surface, the highest point of the dry dome at this time, and just to the east of Amarillo it drops down to near the 900-mb surface in the moist tropical air. The steepest slope appears to be over or slightly to the east of AMA.

Figure 11 shows the wind analysis for this same cross-section with isovels drawn in intervals of 10 knots. It shows three distinct jet maxima intersecting the vertical plane. The subtropical jet stream is near the height of the 150 mb surface, the polar front jet is near the height of the 250 mb surface, and a third maxima is located in the vicinity of the 500 mb surface in a region of maximum slope of the isotherms and

isentropes. This maxima extends eastward over the area between TIK and FSM which show moderately strong convection from surface reports.

The vertical cross-section through the same area at 1800 CST is shown in figs. 12 and 13. The dry dome has now expanded in height to where the highest point of the dome is near the 500 mb surface. At this time the isentrope θ =302 K is near the 500 mb surface over AMA and drops to near the 850 mb surface over TIK and remains at this height eastward to LIT. The wind analysis for 1800 CST shown in fig. 13 also indicates multiple jet maxima intersecting the vertical plan; the subtropical jet near the 225 mb surface, the polar front jet near the 300 mb surface, and a third jet near the 400 mb surface above the line of convective activity east of TIK. One other feature shown in the wind analysis is that just above the dry dome over AMA the wind increases from 48 to 84 knots through the temperature inversion about 2000 feet in thickness.

5. Summary and Conclusions

This study has shown that mesoscale phenomena such as dry fronts can be observed on ATS pictures soon after they form and their development and motion can be determined from consecutive pictures. Although this specific dry front did not initiate very severe thunderstorm and/or tornado activity, there are numerous cases when such activity did occur. Therefore it is important for such lines to be detected as early as possible from the forecaster's point of view. However, the three dimensional structure of such systems can best be determined by combining conventional upper air data and radar pictures with the ATS pictures.

REFERENCES

Beebe, R. G., 1958: An instability line development as observed by the tornado research plane. J. of Meteor., 15, No. 3, 278-282.

Fujita, T., 1958: Structure and movement of a dry front. Bull. Amer. Meteor. Soc., 39, No. 11, 574-582.

_____, 1966: Early stage of tornado development as revealed by satellite photographs. SMRP Research Paper No. 50, The University of Chicago, 15 pp.

McGuire, E. L., 1962: The vertical structure of three dry lines as revealed by aircraft traverses. National Severe Storms Project Report, No. 7, Weather Bureau, 10 pp.

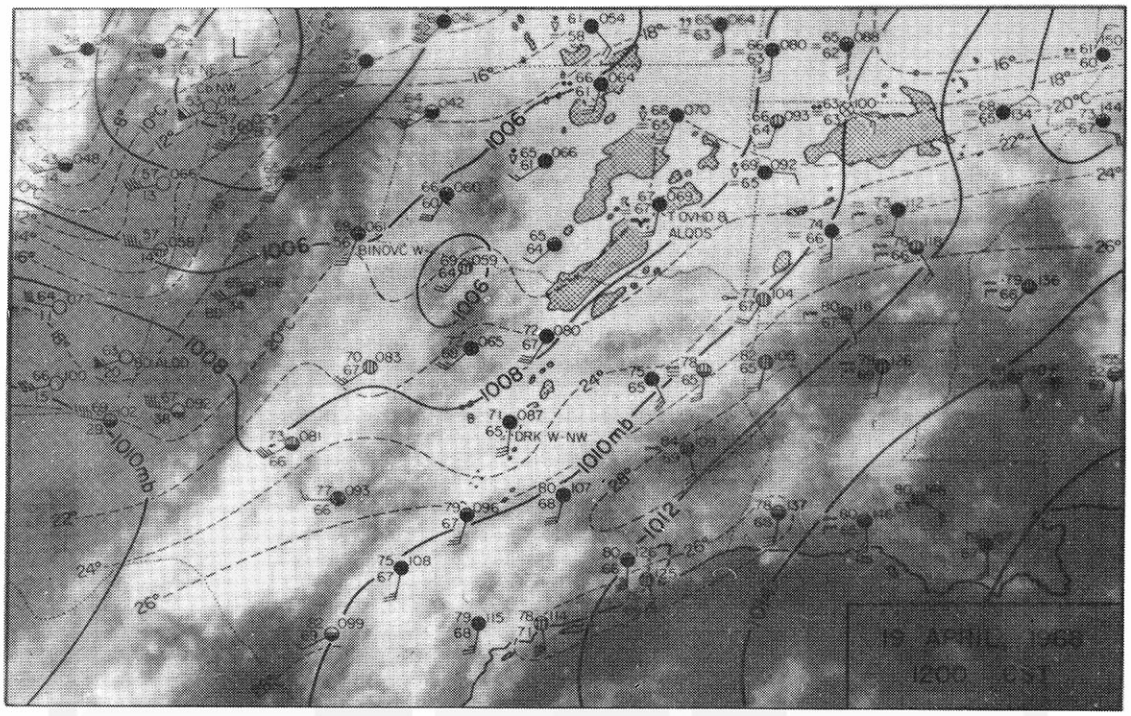

Fig. 1. Surface chart for 1200 CST on 19 April 1968 with isobars (solid lines) and air temperatures (dashed lines). Stippled areas represent composite radar echoes detected at this time. Surface data plotting symbols: ◒ = amt. of low cloud with base < 8000 ft., ◍ = amt. of middle and high cloud with base > 8000 ft., ▲— =25 knots, —\ = 5 knots.

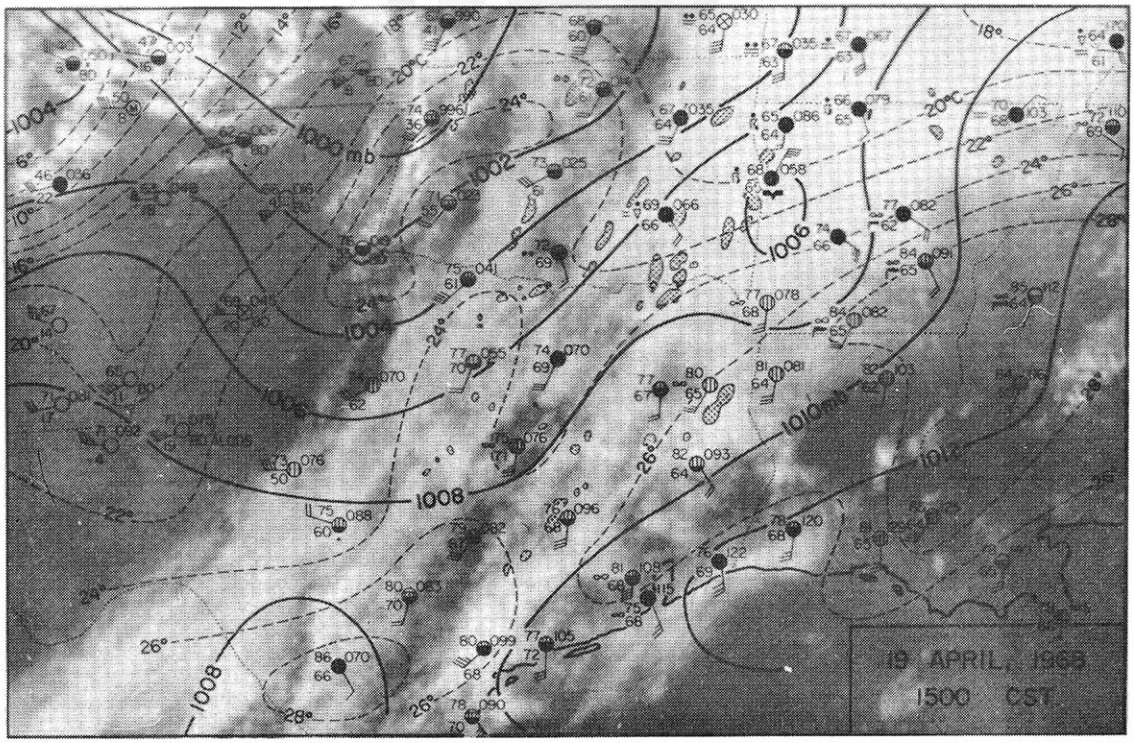

Fig. 2. Surface chart for 1500 CST on 19 April 1968 with isobars (solid lines) and air temperatures (dashed lines). Stippled areas represent composite radar echoes detected at this time. Surface data plotting symbols: same as for Fig. 1.

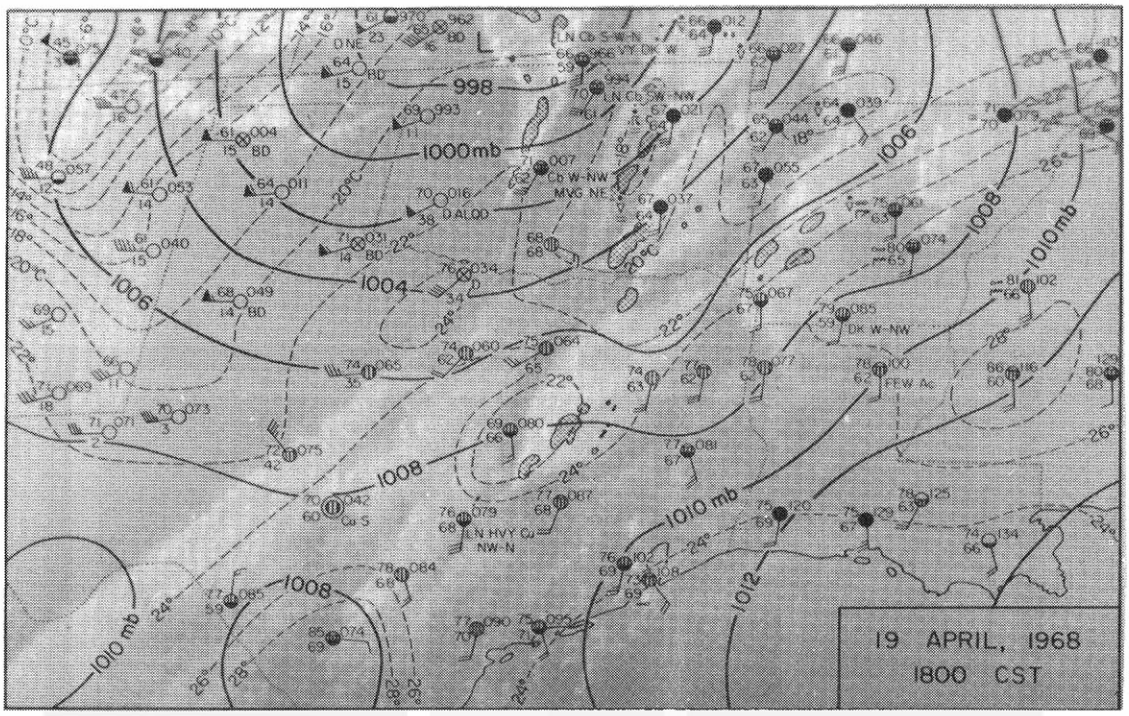

Fig. 3. Surface chart for 1800 CST on 19 April 1968 with isobars (solid lines) and air temperatures (dashed lines). Stippled areas represent composite radar echoes. Surface data plotting symbols: Same as for fig. 1.

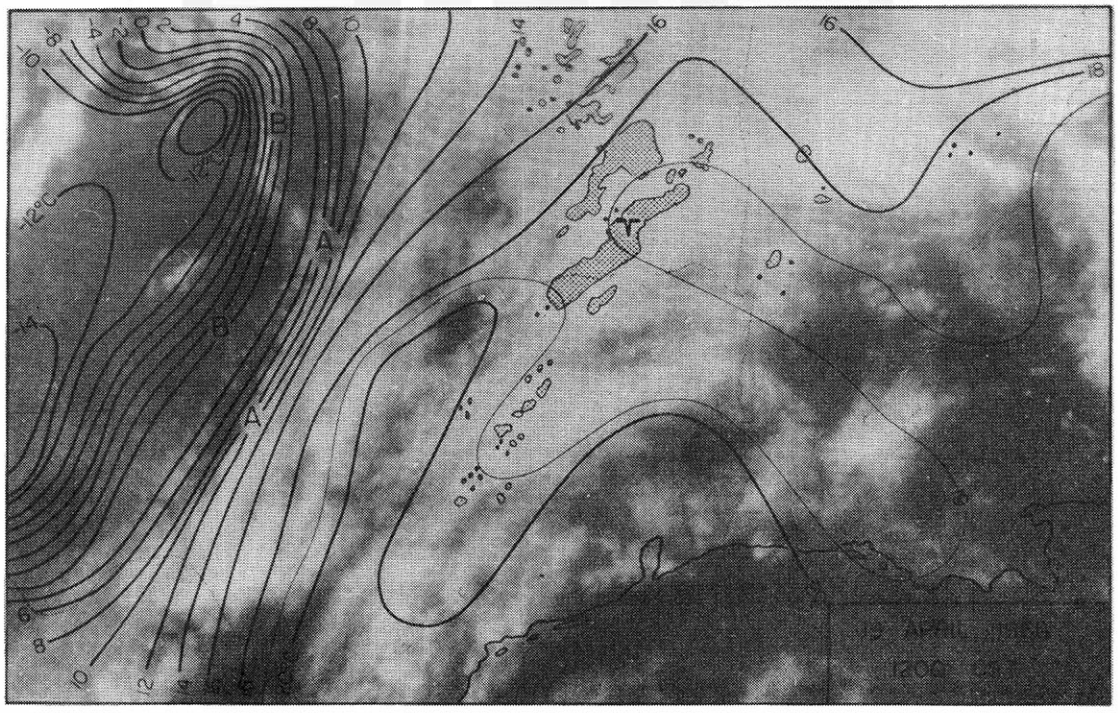

Fig. 4. A portion of ATS III cloud picture taken at 1203 CST on 19 April 1968 with composite radar echoes indicated by stippled areas. Surface isodrosotherms are drawn for 2C intervals and the two dry line zones are indicated by A-A and B-B. The large radar echo over north central Arkansas (shown in Fig. 1) was omitted from this figure since it does not relate to any severe convective activity.

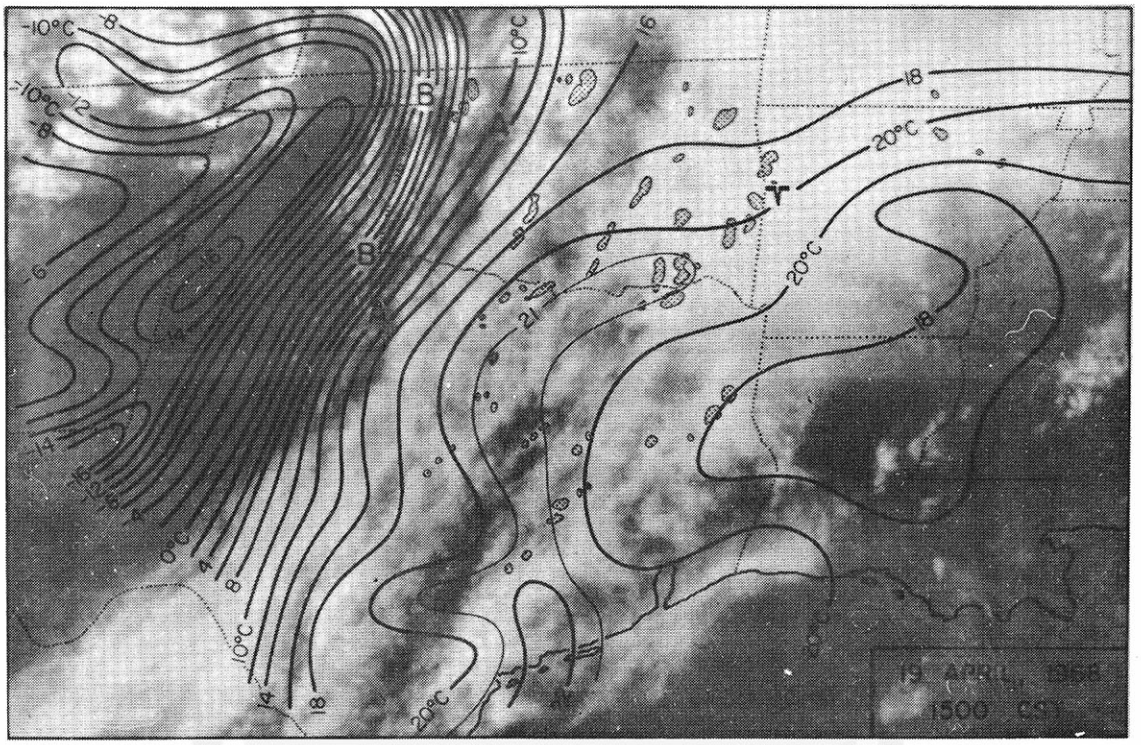

Fig. 5. A portion of ATS III cloud picture taken at 1503 CST on 19 April 1968 with composite radar echoes indicated by stippled areas. Surface isodrosotherms are drawn for 2C intervals and the two dry line zones are indicated by A-A and B-B.

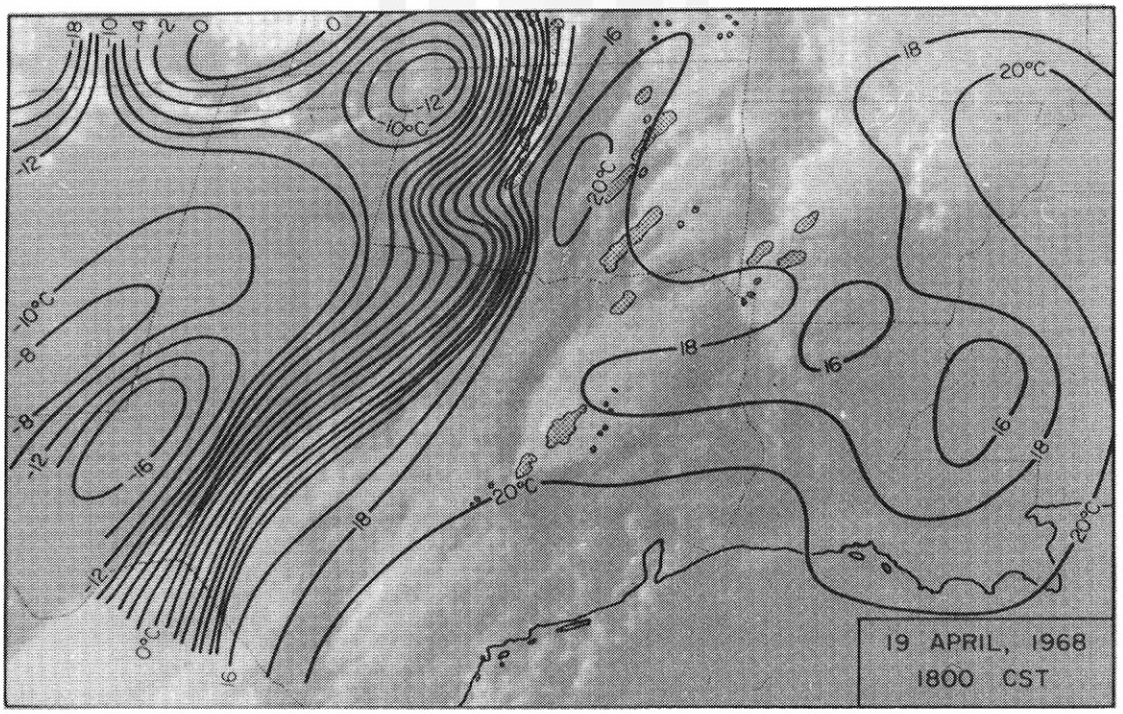

Fig. 6. A portion of ATS III cloud picture taken at 1805 CST on 19 April 1968 with composite radar echoes indicated by stippled areas. Surface isodrosotherms are drawn for 2C intervals. The two dry lines are nearly merged into one wide zone just west of OKC.

FIG 7

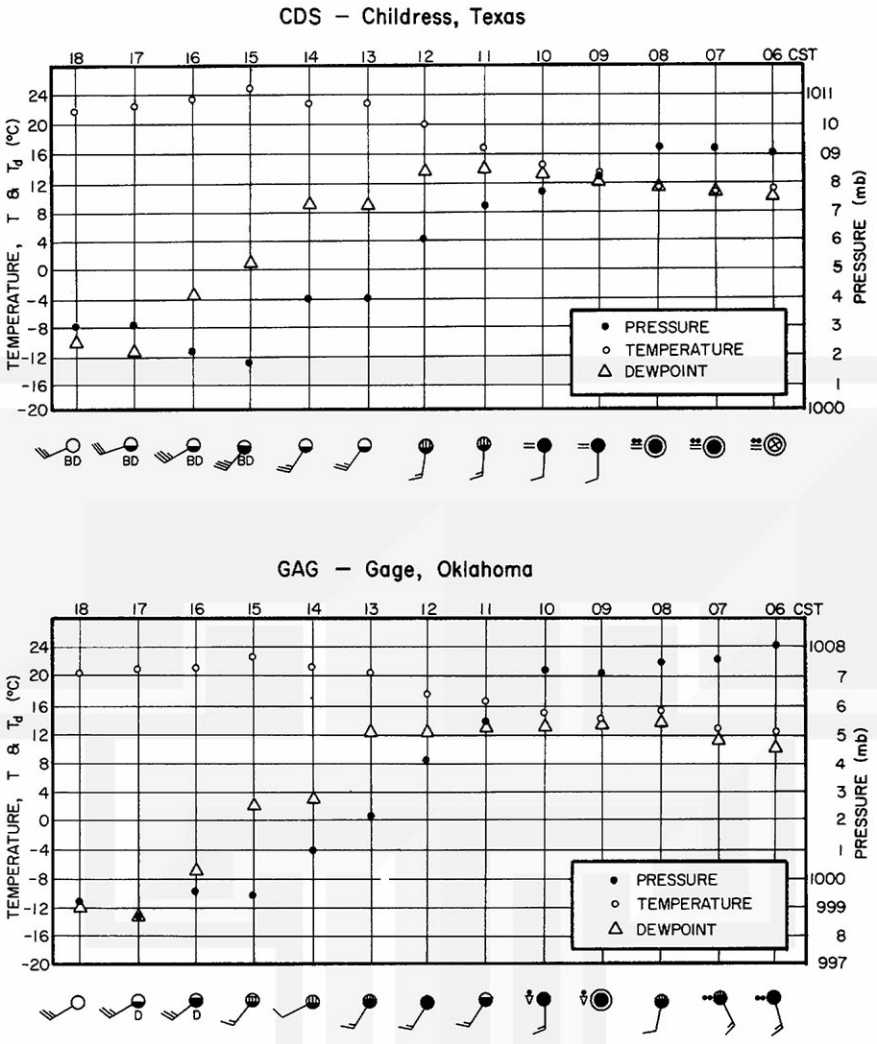

Fig. 7. Time section of pressure (in mb), air temperature (deg C) and dew-point temperature (deg C) for Childress, Texas and Gage, Oklahoma between 0600 and 1800 CST on 19 April 1968. Both dry lines A-A and B-B passed over these stations during the afternoon hours.

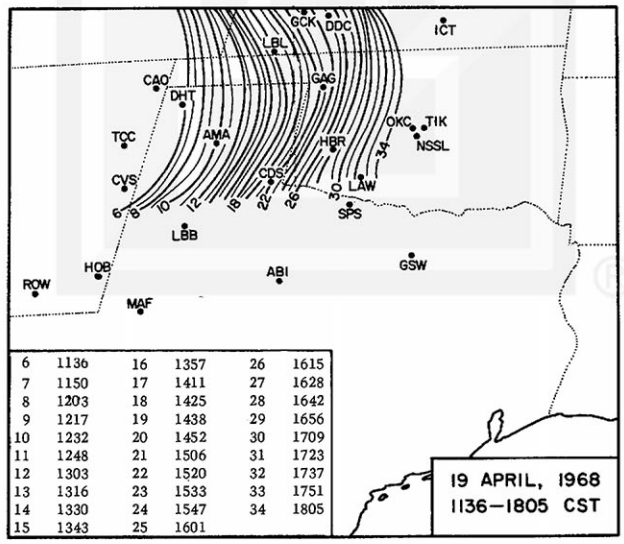

Fig. 8. Consecutive positions of dry line B-B determined from ATS III cloud picture frames 6 through 34 taken between 1136 and 1805 CST on 19 April 1968. The picture time is beginning picture time plus 6 minutes.

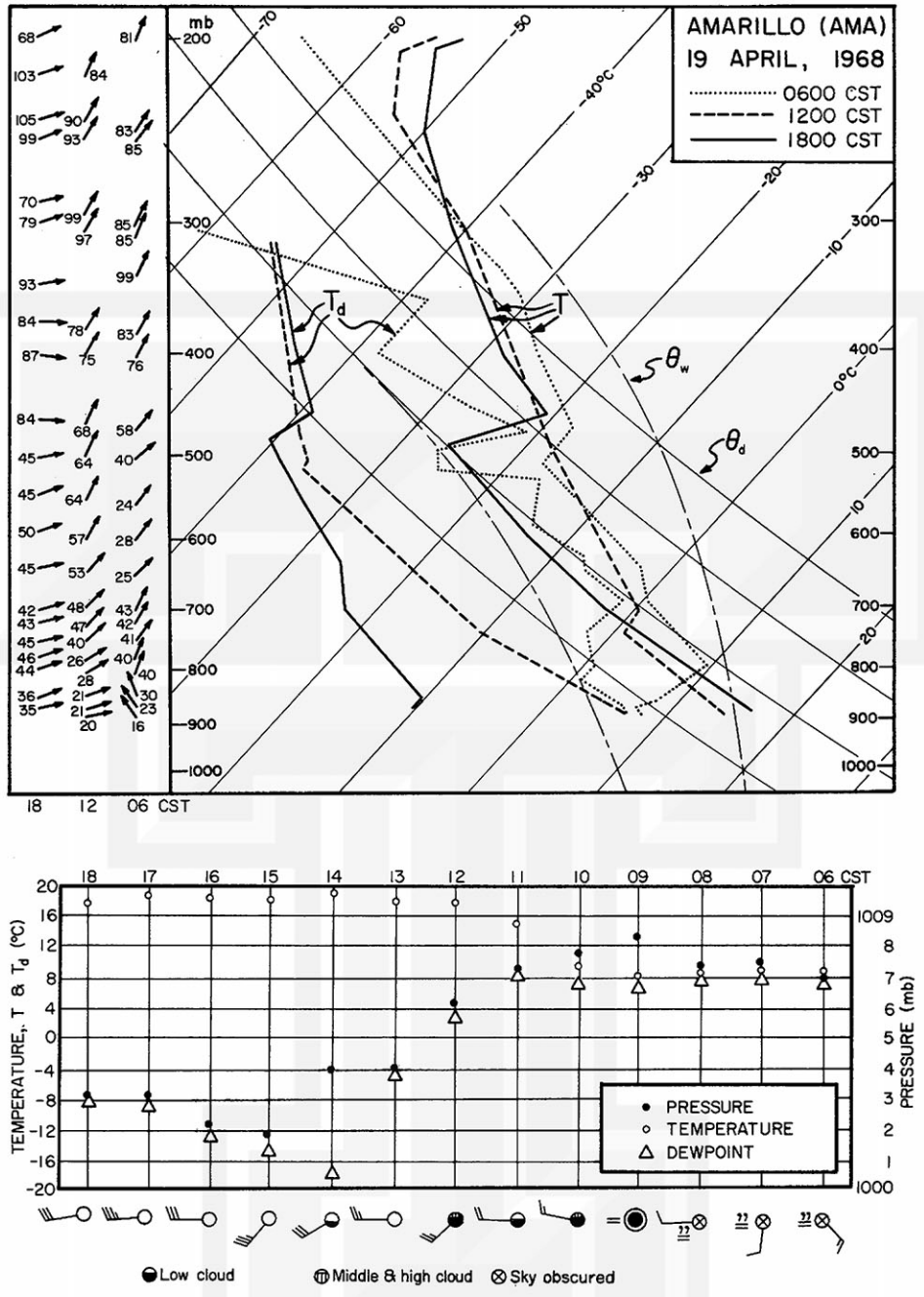

Fig. 9. Upper part: Three pressure-temperature and pressure-humidity curves for Amarillo, Texas on 19 April 1968. The corresponding upper winds are indicated in the left margin of the graph.

Lower part: Time section of pressure, air temperature and dew-point temperature reported at Amarillo between 0600 and 1800 CST. Cloud cover and surface winds are also indicated. The numbers opposite the wind shafts are reported wind speeds in knots.

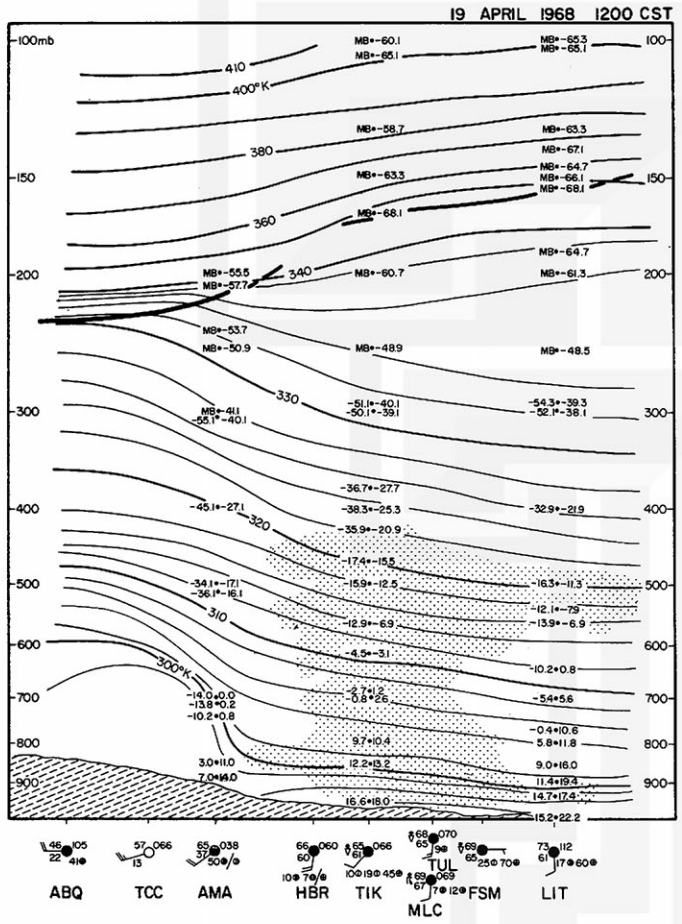

Fig. 10. Vertical cross-section between Little Rock, Arkansas (LIT) and Albuquerque, New Mexico (ABQ) at 1200 CST on 19 April 1968 with air temperatures and dew-point temperatures plotted. Heavy lines indicate tropopauses. Isentropes are drawn for every 2 degrees K from the ground up to the 340 K level and then for every 10 degrees K up to the 100 mb level.

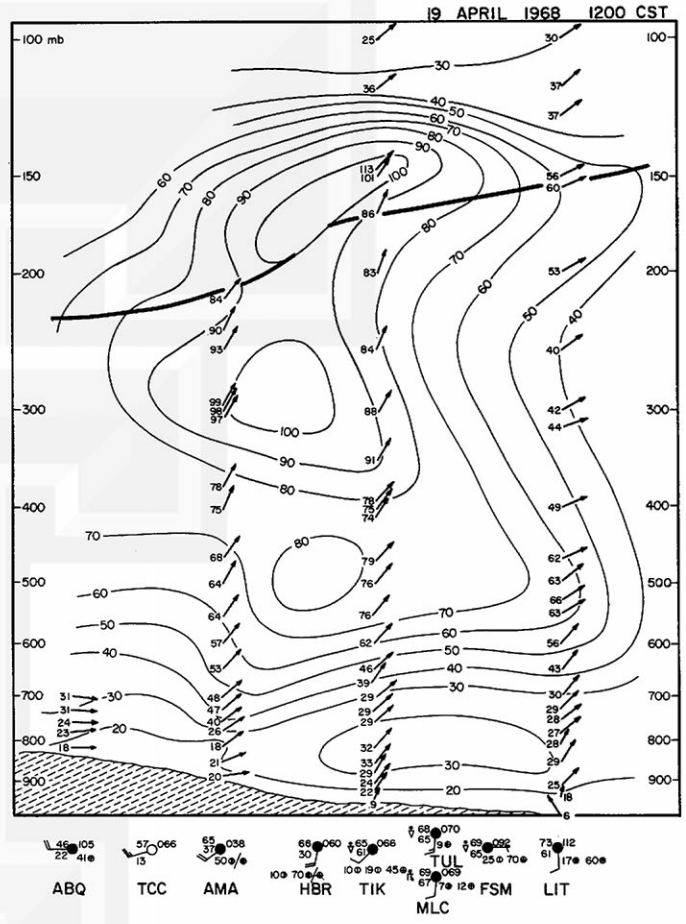

Fig. 11. Vertical cross-section between Little Rock, Arkansas (LIT) and Albuquerque, New Mexico (ABQ) at 1200 CST on 19 April 1968 with upper winds plotted. Heavy line indicates tropopause. Isovels are drawn for every 10 knots.

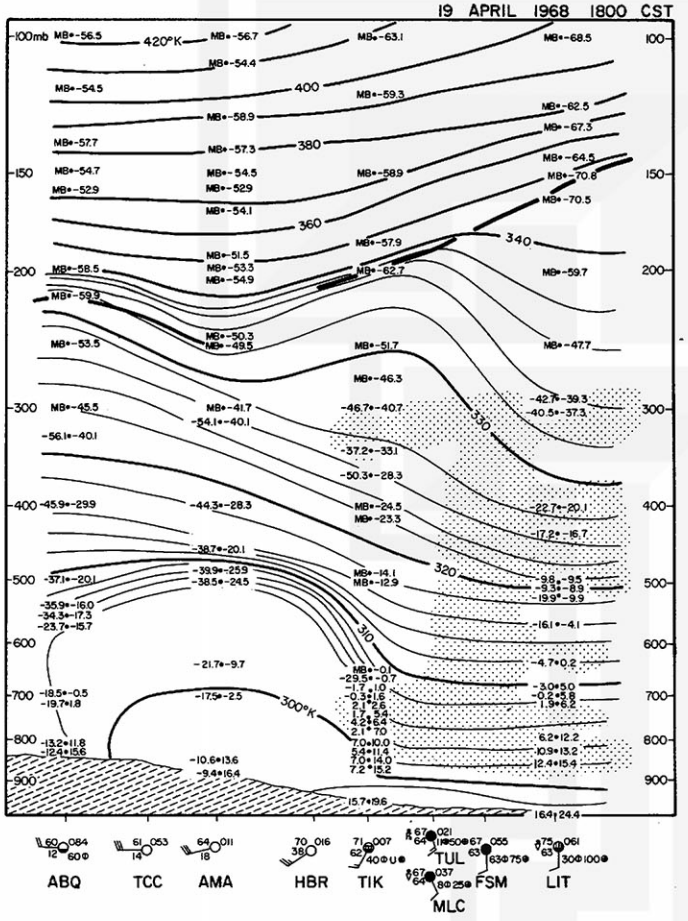

Fig. 12. Vertical cross-section between Little Rock, Arkansas (LIT) and Albuquerque, New Mexico (ABQ) at 1800 CST on 19 April 1968 with air temperatures and dew-point temperatures plotted. Heavy line represents the tropopause. Isentropes are drawn for every 2 degrees K from the ground up to the 340 K and then for every 10 degrees K to the 100 mb level.

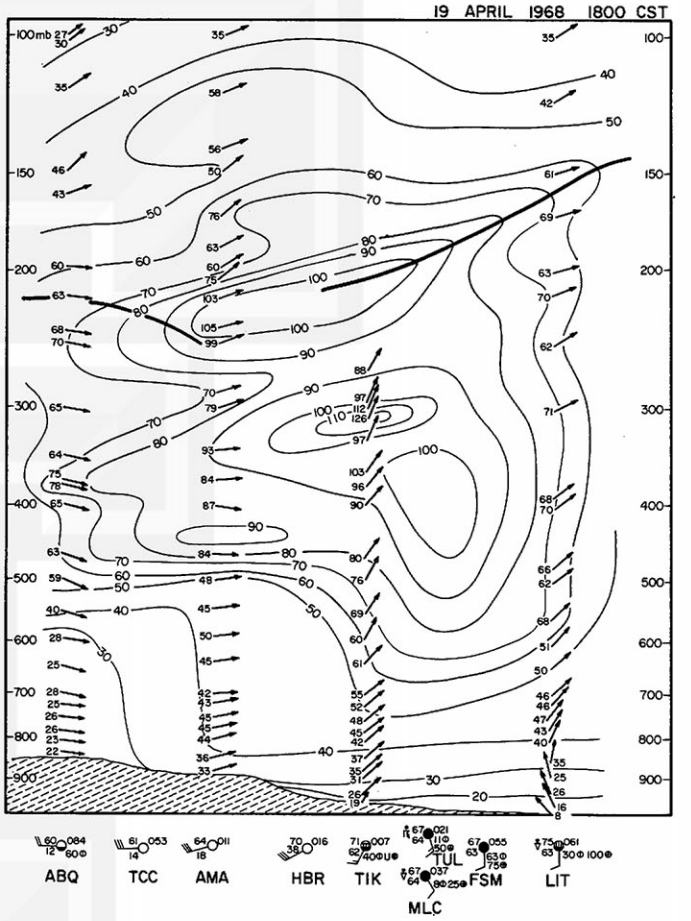

Fig. 13. Vertical cross-section between Little Rock, Arkansas (LIT) and Albuquerque, New Mexico (ABQ) at 1800 CST on 19 April 1968 with upper wind data plotted. Heavy line represents the tropopause. Isovels are drawn for every 10 knots.

MESOMETEOROLOGY PROJECT - - - RESEARCH PAPERS

(Continued from front cover)

42.* A Study of Factors Contributing to Dissipation of Energy in a Developing Cumulonimbus - Rodger A. Brown and Tetsuya Fujita

43. A Program for Computer Gridding of Satellite Photographs for Mesoscale Research - William D. Bonner

44. Comparison of Grassland Surface Temperatures Measured by TIROS VII and Airborne Radiometers under Clear Sky and Cirriform Cloud Conditions - Ronald M. Reap

45. Death Valley Temperature Analysis Utilizing Nimbus I Infrared Data and Ground-Based Measurements - Ronald M. Reap and Tetsuya Fujita

46. On the "Thunderstorm-High Controversy" - Rodger A. Brown

47. Application of Precise Fujita Method on Nimbus I Photo Gridding - Lt. Cmd. Ruben Nasta

48. A Proposed Method of Estimating Cloud-top Temperature, Cloud Cover, and Emissivity and Whiteness of Clouds from Short- and Long-wave Radiation Data Obtained by TIROS Scanning Radiometers - T. Fujita and H. Grandoso

49. Aerial Survey of the Palm Sunday Tornadoes of April 11, 1965 - Tetsuya Fujita

50. Early Stage of Tornado Development as Revealed by Satellite Photographs - Tetsuya Fujita

51. Features and Motions of Radar Echoes on Palm Sunday, 1965 - D. L. Bradbury and T. Fujita

52. Stability and Differential Advection Associated with Tornado Development - Tetsuya Fujita and Dorothy L. Bradbury

53. Estimated Wind Speeds of the Palm Sunday Tornadoes - Tetsuya Fujita

54. On the Determination of Exchange Coefficients: Part II - Rotating and Nonrotating Convective Currents - Rodger A. Brown

55. Satellite Meteorological Study of Evaporation and Cloud Formation over the Western Pacific under the Influence of the Winter Monsoon - K. Tsuchiya and T. Fujita

56. A Proposed Mechanism of Snowstorm Mesojet over Japan under the Influence of the Winter Monsoon - T. Fujita and K. Tsuchiya

57. Some Effects of Lake Michigan upon Squall Lines and Summertime Convection - Walter A. Lyons

58. Angular Dependence of Reflection from Stratiform Clouds as Measured by TIROS IV Scanning Radiometers - A. Rabbe

59. Use of Wet-beam Doppler Winds in the Determination of the Vertical Velocity of Raindrops inside Hurricane Rainbands - T. Fujita, P. Black and A. Loesch

60. A Model of Typhoons Accompanied by Inner and Outer Rainbands - Tetsuya Fujita, Tatsuo Izawa., Kazuo Watanabe and Ichiro Imai

61. Three-Dimensional Growth Characteristics of an Orographic Thunderstorm System - Rodger A. Brown

62. Split of a Thunderstorm into Anticyclonic and Cyclonic Storms and their Motion as Determined from Numerical Model Experiments - Tetsuya Fujita and Hector Grandoso

63. Preliminary Investigation of Peripheral Subsidence Associated with Hurricane Outflow - Ronald M. Reap

64. The Time Change of Cloud Features in Hurricane Anna, 1961, from the Easterly Wave Stage to Hurricane Dissipation - James E. Arnold

65. Easterly Wave Activity over Africa and in the Atlantic with a Note on the Intertropical Convergence Zone during Early July 1961 - James E. Arnold

66. Mesoscale Motions in Oceanic Stratus as Revealed by Satellite Data - Walter A. Lyons and Tetsuya Fujita

67. Mesoscale Aspects of Orographic Influences on Flow and Precipitation Patterns - Tetsuya Fujita

68. A Mesometeorological Study of a Subtropical Mesocyclone -Hidetoshi Arakawa, Kazuo Watanabe, Kiyoshi Tsuchiya and Tetsuya Fujita

69. Estimation of Tornado Wind Speed from Characteristic Ground Marks - Tetsuya Fujita, Dorothy L. Bradbury and Peter G. Black

70. Computation of Height and Velocity of Clouds from Dual, Whole-Sky, Time-Lapse Picture Sequences - Dorothy L. Bradbury and Tetsuya Fujita

71. A Study of Mesoscale Cloud Motions Computed from ATS-I and Terrestrial Photographs - Tetsuya Fujita, Dorothy L. Bradbury, Clifford Murino and Louis Hull

72. Aerial Measurement of Radiation Temperatures over Mt. Fuji and Tokyo Areas and Their Application to the Determination of Ground- and Water-Surface Temperatures - Tetsuya Fujita, Gisela Baralt and Kiyoshi Tsuchiya

73. Angular Dependence of Reflected Solar Radiation from Sahara Measured by TIROS VII in a Torquing Maneuver - Rene Mendez.

74. The Control of Summertime Cumuli and Thunderstorms by Lake Michigan During Non-Lake Breeze Conditions - Walter A. Lyons and John W. Wilson

75. Heavy Snow in the Chicago Area as Revealed by Satellite Pictures - James Bunting and Donna Lamb

76. A Model of Typhoons with Outflow and Subsidence Layers - Tatsuo Izawa

* out of print

(continued on outside back cover)

MESOMETEOROLOGY PROJECT - - - RESEARCH PAPERS

(Continued from inside back cover)

77. Yaw Corrections for Accurate Gridding of Nimbus HRIR Data - Roland A. Madden

78. Formation and Structure of Equatorial Anticyclones Caused by Large-Scale Cross Equatorial Flows Determined by ATS-I Photographs - Tetsuya T. Fujita and Kazuo Watanabe and Tatsuo Izawa

79. Determination of Mass Outflow From a Thunderstorm Complex Using ATS III Pictures - T. T. Fujita and D. L. Bradbury